



ELSEVIER

Available online at [www.sciencedirect.com](http://www.sciencedirect.com)



Physics Procedia 3 (2010) 685–689

**Physics  
Procedia**

[www.elsevier.com/locate/procedia](http://www.elsevier.com/locate/procedia)

International Congress on Ultrasonics, Universidad de Santiago de Chile, January 2009

## Vector Component Focusing in Elastic Solids using a Scalar Source in Three Component Time Reversal

Koen Van Den Abeele<sup>a\*</sup>, TJ Ulrich<sup>b</sup>, Pierre-Yves Le Bas<sup>b</sup>, Michele Griffa<sup>b</sup>, Brian E.  
Anderson<sup>b</sup>, Robert A. Guyer<sup>b</sup>

<sup>a</sup>*Katholieke Universiteit Leuven - Campus Kortrijk, Wave Propagation and Signal Processing Research Group,  
E. Sabbelaan 53, B-8500 Kortrijk, Belgium*

<sup>b</sup>EES-11, Los Alamos National Laboratory, Los Alamos, New Mexico 87545, USA

---

### Abstract

This contribution provides fundamental support, and both experimental and numerical wave propagation results demonstrating the ability to use a scalar source, a three component detector and the reciprocal TR process to selectively focus different vector components, either individually or collectively. The principle is explained from an analytical point of view, and the numerical and experimental study demonstrates excellent temporal and spatial focalization. Applications of the selective vector component focusing can be found in damage imaging techniques using both linear or nonlinear ultrasonic waves.

*Keywords:* Time Reversal; imaging; focusing.

---

### 1. Introduction

In acoustics (dealing with sound waves in fluids or gases), it is known that, for a given response signal at an arbitrary location, reciprocity and Time Reversal (TR) can be used to focus high levels of acoustic energy at that position. In the case of elastic solids, sound waves generally induce different disturbances in three directions. The propagation of an initial scalar disturbance in a solid converts to different types of wave motion (i.e., shear and compressional) upon encountering scatterers and boundaries, and results in a wave field composed of motion in each of the three spatial directions, interrelated to different types of wave motion. Traditionally in TR studies the vector components of the wave field are generally disregarded, either due to the scalar nature of propagating waves in acoustic media (i.e., fluids) or due to the difficulty of measuring components other than the normal (relative to the sample surface) of the wave field in elastic media (i.e., solids). With the advent of TR based techniques in solids [1-4] the ability to exploit the vector nature of elastic waves in solids may prove useful in nondestructive testing (NDT)

---

\* Corresponding author. Tel.: +32 56 246 256; fax: +32 56 246 999.  
E-mail address: [koen.vandenabeele@kuleuven-kortrijk.be](mailto:koen.vandenabeele@kuleuven-kortrijk.be)

and other yet to be developed applications. We will show that reciprocal TR [1-2] can be used to focus energy in solids in any direction by selecting a scalar combination of the vectorial components.

## 2. Background

In order to illustrate the idea of selective vector component focusing, we assume the following experiment and translate it into analytical expressions: Consider a 3D object of arbitrary geometry with a source location  $A$  and receiver location  $B$ , each with their own right hand cartesian coordinate system  $X_A$  and  $X_B$  and unit vectors  $\mathbf{e}_x, \mathbf{e}_y, \mathbf{e}_z$ , and  $\mathbf{e}_x', \mathbf{e}_y', \mathbf{e}_z'$ , respectively. A source function with spectrum  $F^{(1)}(\omega)$  is broadcast at the origin of  $X_A$  with a transducer that produces forces in the direction  $\mathbf{e}_x$ . The three components of the displacement field are received at  $X_B$ . Using Green's function theory, the spectrum of the detected displacement fields can be expressed as follows:

$$R_{\alpha'}^{(1)}(\omega; B) = \sum_{\alpha} (\bar{\mathbf{e}}_{\alpha'} \cdot \bar{\mathbf{e}}_{\alpha}) G_{\alpha\alpha'}(B|A) F^{(1)}(\omega).$$

with  $\alpha$  representing the  $x, y$  and  $z$  components and the Green functions  $G_{xx}, G_{yx}, G_{zx}$  are written in terms of the source coordinate system. Subsequently, we time reverse the three detected displacement fields separately and make an arbitrary linear *scalar* combination of these components to produce a second *scalar* source time function with spectrum

$$F^{(2)}(\omega) = \sum_{\alpha'} a_{\alpha'} \tilde{R}_{\alpha'}^{(1)*}(\omega; B) = \sum_{\alpha', \alpha} a_{\alpha'} (\bar{\mathbf{e}}_{\alpha'} \cdot \bar{\mathbf{e}}_{\alpha}) G_{\alpha\alpha'}^*(B|A) F^{(1)*}(\omega).$$

where the asterisk stands for the complex conjugate of the frequency spectrum, which corresponds to the time reversal manipulation in the time domain. We now broadcast the second source time function from  $A$  using the same initial transducer that produces forces in the  $\mathbf{e}_x$  direction. The three components of the displacement field received at  $B$  are:

$$R_{\beta'}^{(2)}(\omega; B) = \sum_{\beta} (\bar{\mathbf{e}}_{\beta'} \cdot \bar{\mathbf{e}}_{\beta}) G_{\beta\alpha'}(B|A) F^{(2)}(\omega).$$

If we consider for simplicity the case in which the primed and unprimed coordinate systems are the same, apart from a translation, then

$$R_{\beta'}^{(2)}(\omega; B) = \sum_{\alpha} a_{\alpha} G_{\beta\alpha}(B|A) G_{\alpha\alpha'}^*(B|A) F^{(1)*}(\omega).$$

As cross terms, such as,

$$G_{\beta\alpha}(B|A) G_{\alpha\alpha'}^*(B|A)$$

with  $\alpha \neq \beta$  are negligible, i.e., they do not contribute constructively to the TR focus, the received spectra for the three components after reciprocal TR [1-2] can be expressed as follows:

$$R_x^{(2)}(\omega; B) \approx a_x G_{xx}(B|A) G_{xx}^*(B|A) F^{(1)*}(\omega)$$

$$R_y^{(2)}(\omega; B) \approx a_y G_{yx}(B|A) G_{yx}^*(B|A) F^{(1)*}(\omega)$$

$$R_z^{(2)}(\omega; B) \approx a_z G_{zx}(B|A) G_{zx}^*(B|A) F^{(1)*}(\omega)$$

which clearly implies that a scalar energy source can be used to focus in three directions, either individually or combined.

### 3. Numerical and Experimental verification

To complement the above discussed analytical results which are expressed in the frequency domain, we carried out a numerical and experimental study of the selective vector component focusing in the time domain. The 3D wave propagation model used in the simulations is based on the staggered grid Elastodynamic Finite Integration Technique (EFIT) [5]. For the experiments we used a small piezoelectric disk (d33 polarized PZT-5,  $d = 12$  mm,  $h = 2$  mm) for excitation, and non-contact laser vibrometry for detection. The velocity measurements of the three vector components  $v_x$ ,  $v_y$ , and  $v_z$  were achieved using two Polytec laser vibrometers, the OFV 303 (3001 controller, VD-02, 25 mm/s/V) for the normal ( $z$ ) component and the OFV 552 (5000 controller, VD-02, 25 mm/s/V) fiber-optic differential laser vibrometer (DLV) for the in-plane ( $x$  and  $y$ ) components. To obtain the in-plane components using the DLV the two fiber-optic laser heads were placed at  $\pm 30^\circ$  from vertical such that the normal component is eliminated, thus leaving only the in-plane component.

The simulations and experiments are performed on a cube sample of fused silica-type material (dimensions  $10 \times 10 \times 10$  cm<sup>3</sup>,  $v_c \approx 6000$  m/s,  $v_s \approx 2700$  m/s,  $Q \approx 1500$ ,  $\rho \approx 2500$  kg/m<sup>3</sup>). As the first source, a short pulse with a frequency of 200kHz is considered which is excited on the ( $y$ - $z$ ) plane ( $x=0$  cm), with an assumed exclusively out-of plane motion in the  $x$ -direction. The three particle velocity components  $v_x$ ,  $v_y$ , and  $v_z$  at an arbitrary receiving location in the ( $x$ - $y$ ) plane (at  $z=10$  cm) are subsequently used for reciprocal TR, either individually or combined.

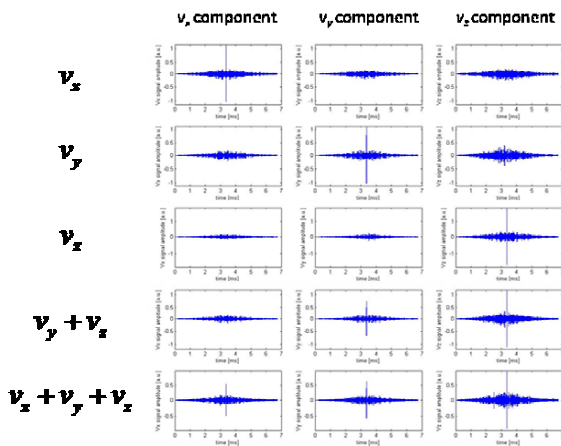


Fig.1 Numerical simulations of the selective focusing after reciprocal TR of individual particle velocity components and of various combinations. Left column specifies the scalar input information supplied to the source for rebroadcasting at position A. Right column displays the subsequent recording of the three particle velocity components at location B.

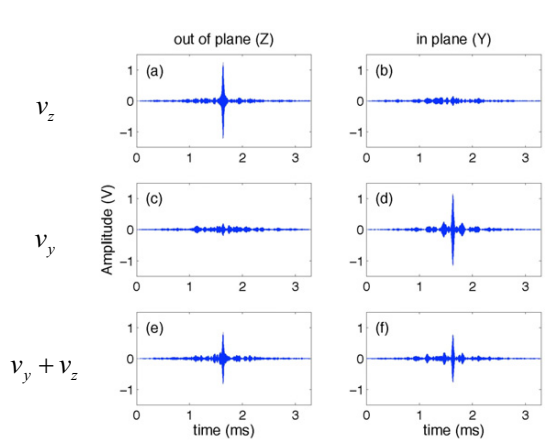


Fig.2 Same as in Figure 1, but for experiments.

Figure 1 (simulation) and Figure 2 (experimental) give an overview of the time signals (temporal focusing) at the receiver for each of the three components when only  $v_x$ ,  $v_y$ ,  $v_z$ , or combinations such as  $v_y+v_z$  and  $v_x+v_y+v_z$  are considered in the rebroadcast signal. In all cases, it is clear that the TR procedure allows the scalar information which is supplied to the source to be separated into the correct vector components. For instance, when  $v_y+v_z$  is considered as input signal, the time reversed signal will redistribute and focus the energy in the  $y$  and  $z$  direction at the receiving point, without focusing at the  $x$ -direction.

Figure 3 illustrates the spatial focusing of the three components in a  $40 \times 40$  mm<sup>2</sup> scanning area of the ( $x$ - $y$ ) plane around the receiver location when the scalar combination  $v_x+v_y+v_z$  is considered in the rebroadcast signal. We note a

near identical focal structure for each component, indicating a highly effective localization of energy in each of the three dimension.

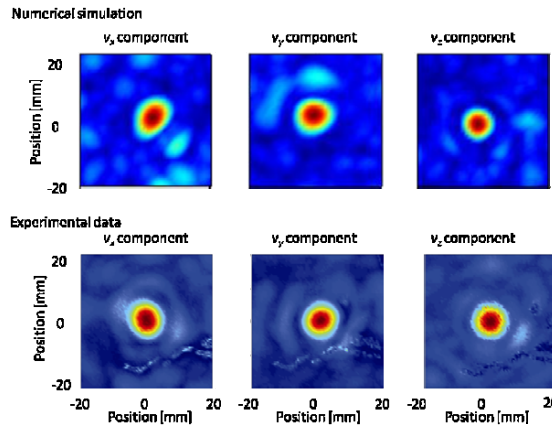


Fig.3 Three component focusing with  $v_x+v_y+v_z$ . Model results (Top row) and experimental results (Bottom row). Magnitude of the three velocity components of motion. The color scales are normalized to the maximum amplitude in each respective component. Note the near identical focal structure for each component. The segmented ribbon-like feature in the lower half of the images is a region of impaired reflectivity for the laser vibrometers and does not represent any physical structure of the medium.

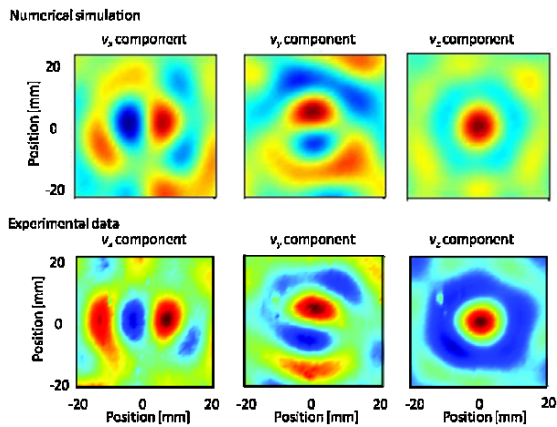


Fig.4 Single component focusing with  $v_z$ . Model results (Top row) and experimental results (Bottom row). Instantaneous motion at focal time of three velocity components of motion. Note the dipole motion seen in the in-plane components around the focal location due to the Poisson effect.

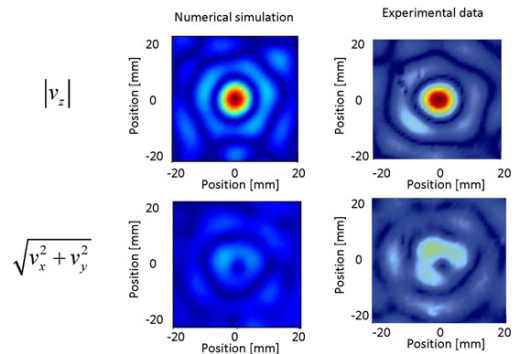


Fig.5 Single component focusing with  $v_z$ . Model results (left column) and experimental results (Right column). (a) Out of plane and (b) in-plane magnitudes. (a) and (b) use the same color scale to accurately depict the relative amplitudes of the in-plane and out of plane components at the time of focus. The Poisson effect is manifest in the in-plane components around the focal location.

Spatial focusing using a single component reciprocal TR procedure is illustrated in Figures 4 and 5. In this case only the out of plane ( $z$ ) component is used in the reciprocal TR process. Again, we provide images of a scan (simulation and experiment) along the surface in the ( $x$ - $y$ ) plane around the receiver position. This time we visualize the values at the focal time for each velocity component. The color scales are normalized to the maximum amplitude in each respective component to illustrate the full structure of the vector wave field. Red colors indicate positive motion, blue colors represent negative motion. The in-plane dipole motion seen in the  $v_x$  and  $v_y$  component around the focal location is due to the Poisson effect. In this perspective, the application of reciprocal TR in solids might be thought of as an alternative experimental tool for measuring or monitoring the Poisson coefficient. Figure 5 shows the out of plane and in-plane magnitudes, i.e.,  $|v_z|$  and (b)  $\sqrt{v_x^2 + v_y^2}$  on the same color scale. We observe that the Poisson effect is manifest in the in-plane components around the focal location, however, these amplitudes, while higher than the background, are quite small with respect to the focal amplitude along  $z$  (out of plane).

#### 4. Conclusion

The results presented in this paper provide the proof that information about the vector response at a certain location can be used in reciprocal TR using a scalar source to selectively focus each of the different vector components, either individually or collectively. The proof is composed of an analytical description of this process and both experimental and numerical wave propagation results.

Potential applications of selective focusing can be found in linear and nonlinear ultrasonic NDT to investigate local variations of the Poisson Coefficient, to image surface conditions using selective excitations of in-plane and out-of plane cracks, to construct virtual arrays for subsequent beam steering, etc.

#### Acknowledgements

This work is supported by Institutional Support (Campaign 8 and LDRD) at the Los Alamos National Laboratory. Koen Van Den Abeele gratefully acknowledges the support of the European FP6 Grant AERONEWS (AST-CT-2003-502927), the Flemish Fund for Scientific Research (G.0206.02, G.0554.06, G.0443.07), the Research Council of the Katholieke Universiteit Leuven (OT/07/051, CIF1), and the institutional support of the Los Alamos National Laboratory. The authors are grateful for discussions with colleagues Paul Johnson and Carene Larmat on the topics of Time Reversal and reciprocity.

#### References

- [1] A. Sutin, B. Libbey, V. Kurtenoks, D. Fenneman, and A. Sarvazyan, Proceedings of the SPIE - The International Society for Optical Engineering, 6217 (1), 6217B-1 (2006).
- [2] Ulrich, T. J., Sutin, A. M., Claytor, T., Papin, P., Le Bas, P.-Y., and TenCate, J. A., Applied Phys. Lett., in press (2008).
- [3] C. Larmat, J. Tromp, Q. Liu, and J.-P. Montagner (2008), Time reversal location of glacial earthquakes, J. Geophys. Res., in press. (2008).
- [4] Anderson, B. E., Larmat, C., Gri\_a, M. G., Ulrich T. J., and Johnson, P. A., Acoustics Today, January (2008).
- [5] Fellinger P. , Marklein R. , Langenberg K. J. , Klaholz S. , "Numerical modeling of elastic-wave propagation and scattering with EFIT - Elastodynamic Finite Integration Technique", Wave Motion, 21: 47-66(1995).